

This paper was recommended for publication in revised form by Regional Editor Lian-Ping Wang

FLOW REGIMES IN COMMERCIAL METAL FOAM HAVING 10 PORES PER INCH

Altay Arbak
 Istanbul Technical University
 Istanbul, Turkey

Özer Bağcı
 Istanbul Technical University
 Istanbul, Turkey

*** Nihad Dukhan**
 University of Detroit Mercy
 Detroit, MI, USA

Keywords: thermal development; Darcy; experiment; metal foam; water
** Corresponding author: Phone: +313 993 3285, Fax: +313 993 1187*
E-mail address: nihad.dukhan@udmercy.edu

ABSTRACT

Metal foam- a relatively new class of porous media- has many advantageous properties relevant to many engineering applications. The internal structure of the foam has connected cells each having many ligaments that form a web. In addition, metal foam has very high porosity (often greater than 90%) and a large accessible surface area per unit volume. These properties are relevant to filtration, heat exchange and reactors. Flow regimes, and transition from one to another, are critical for understanding the pumping power for flow through the foam. The current study will shed some light on pressure drop and flow regimes in metal foam. In particular, a large set of experimental data for pressure drop of water flow in commercial open-cell aluminum foam having 10 pores per inch and a porosity of 88.5% was collected. The range of flow Reynolds number covered all important flow regimes. The current data correlated very well using the friction factor based on the square root of the permeability (measured in the Darcy regime) as a function of Reynolds number based on the same length scale. It is shown that the same foam exhibits different values of its permeability and Forchheimer coefficient in different flow regimes. The findings of this study can help in numerical and analytical work concerning flow and heat transfer in commercial open-cell metal foam and other similar foam-like porous media.

INTRODUCTION

Open-cell metal foam are available commercially and are made from aluminum, copper, steel, nickel and others. Several aspects of the foams and their applications have been

covered in [1]. The foams have relatively high thermal conductivity and large surface area density. The web-like internal structure of the foam is conducive to high rate of mixing of fluid flow. Metal foams are thus suitable for heat transfer enhancement [2-4]. Recently, Bağcı et al. [5] presented experimental heat transfer measurements for water flow in metal foam having 20 pores per inch (ppi) [5].

A good understanding of various flow regimes and pressure drop in metal foam, is indispensable for heat transfer and other applications of the foams. For example, flow fields directly affect convection heat transfer, chemical reaction rates, filtration effectiveness and pumping power. Fluid flow in metal foam is a complex phenomenon due to the internal structure of the foam. In order to understand the pressure drop, one must first understand the characteristics of flow regimes in metal foam and the processes of energy losses in each regime. Transition from one regime to another is also important.

Fluid flow in ‘traditional’ porous media has been studied widely, e.g., [6-11]. Metal foam is different from traditional porous media: 1) it has a very high porosity (often greater than 90%), and 2) it has an internal structure in which the open cells are relatively larger than the ligaments surrounding them. Hence, one must be careful not to simply expect well-accepted empirical results for flow in traditional porous media to be completely valid for flow in metal foam.

The study of Beavers and Sparrow [12] is perhaps the earliest, dedicated in part to investigating pressure drop of water in nickel foam. Unfortunately, the porosity and pore density in this study were not reported. In defining the Reynolds number and friction factors, the square root of the permeability was used

as a length scale. A departure from Darcy regime at Reynolds number of order unity was noted [12].

Montillet et al. [13] studied three nickel foams having 45, 60 and 100 pores per inch (ppi). There was a change in flow regimes at Reynolds number, based on an equivalent pore, between 5 and 10. In a review of pressure drop in metal foam, Edouard et al. [14] noted severe divergence of available correlations in terms of predicting pressure drop, permeability and form/inertia coefficient.

Mancin et al. [15] investigated air pressure drop in six samples of aluminum foam. It was apparent that all the data lied within one flow regime (outside the Darcy regime), and did not exhibit any regime change.

Previously published data on flow in metal foam e.g. [2,16-20] contain significant disagreements on the values of the permeability and form drag coefficient, for foams with similar porosities and internal structures. These discrepancies are possibly due to three causes: 1) foam sample size in flow direction used by various researchers [21], 2) foam sample size perpendicular to flow direction [22,23] and 3) overlooking flow regimes encountered in a given experimental data set. The same metal foam exhibits different values of permeability and form drag coefficient in different flow regimes, as was shown by Boomsma and Poulikakos [19] for water flow and by Dukhan and Minjeur [24] for airflow in aluminum foam.

A transition from Darcy to Forchheimer regime was identified by Boomsma and Poulikakos [19] at an average water velocity around 0.10, 0.11 and 0.07 m/s (Reynolds number based on Darcy-regime permeability 26.5, 22.3 and 14.2) for 10-, 20- and 40-ppi aluminum foam, respectively. In an experimental study, Zhong et al. [22] reported departure from the Darcy regime at Re of about 0.1 for airflow in sintered metal foam. For various metal foams, Bonnet et al. [25] and Liu et al. [26] identified a transition from Darcy to Forchheimer regime. Dukhan and Ali [27] presented results of an experimental study of airflow through aluminum foam samples. A distinction was made between transition from Darcy to Forchheimer regimes and from laminar to turbulent flow regimes.

A series of studies on pressure drop and flow regimes in metal foam started two years ago by the current research team. The first paper generated from this work provided pressure drop and flow regimes for water flow in metal foam having 20 ppi [28]. The current work presents new set of experimental data for water flow in 10-ppi metal foam to establish the various flow regimes in this particular foam. Understanding flow regimes and their boundaries can directly aid numerical and analytical work of flow in metal foam; and it can assist in interpreting heat and mass transport in such media.

EXPERIMENT

The test section was made from an aluminum pipe having an inner diameter of 50.80 mm and a length of 305 mm (Fig. 1). Commercial open-cell aluminum foam, manufactured by ERG Materials and Aerospace, which had 10 ppi (pores per inch) and a porosity of 88.5%, was brazed to the inside surface of the tube.

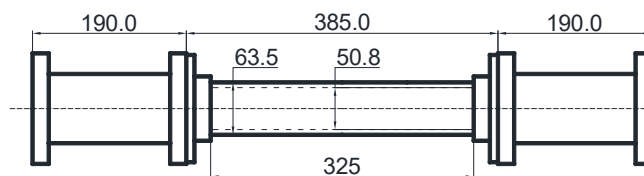


Figure 1. Test section: 1. polyethylene tubes, 2. tube with metal foam, 3. aluminum flanges for connecting the metal foam to the polyethylene tubes (all dimensions are in millimeters).

The rest of the experimental setup used in this study is shown schematically in Fig. 2. Two 50.8-mm-diameter 190-mm-long Polyethylene tubes were connected to the two ends of the test section via specially-designed flanges. Pressure taps were drilled in the Polyethylene tubes. The outlets of the Polyethylene tubes were connected to stainless steel pipes 32 mm in diameter and 110 cm in length. A hose and a valve connected the outlet of one steel pipe to 50-liter tank for collecting water, over a known periods of time, for calculating mass flow rates.

A plastic tank (diameter 41 cm, height 44 cm) was elevated 3.5 m. The tank had 4 discharge points located at a height of 33.2 cm with respect to its bottom. Those outlets helped maintain a constant water height of about 33.2 cm in the tank at all times; this tank was used to supply water with constant pressure to the test section. Heavily filtered tap water was supplied to the tank.

To supply constant-pressure flow to the porous medium, one end of another 1.90-cm hose was connected at 3.1 cm from the bottom of the tank, while the other end was connected to the plumbing containing the aluminum-foam test section. This arrangement provided a constant water height of 33.2 cm in the tank during each experimental run. The experimental rig was able to produce and hold very low water speeds (starting at 5.4×10^{-5} m/s). For high flow rates, water was supplied to the test section using a pump which produced average velocities of up to 0.35 m/s.

The pressure drop was measured by two Validyne pressure-differential sensors, model DP15 and DP45. Each sensor could accommodate diaphragms having different thicknesses, each suitable for a certain pressure-difference ranges. Each sensor was connected to a Validyne CD15 carrier demodulator, which provided zero to 10 V DC signal. The demodulator was connected to a multimeter where the voltage signals were read. Each sensor/diaphragm combination had to be calibrated prior to its use.

For a given run, control valves were adjusted and water was allowed to flow into the foam until steady state was reached. Care was taken as to remove air bubbles from the system by dismantling and reassembling parts of the set-up. At steady state and for a fixed flow rate, water exiting the test section was captured in the collecting tank over a known period of time: approximately 1 to 1.5 minutes for high flow rates, and 3 to 4 minutes for low flow rates. The reason for this difference was that the collecting tank became almost full in the given periods.

Typically five successive voltage readings were taken during collecting a certain mass of water. These readings were recorded and averaged.

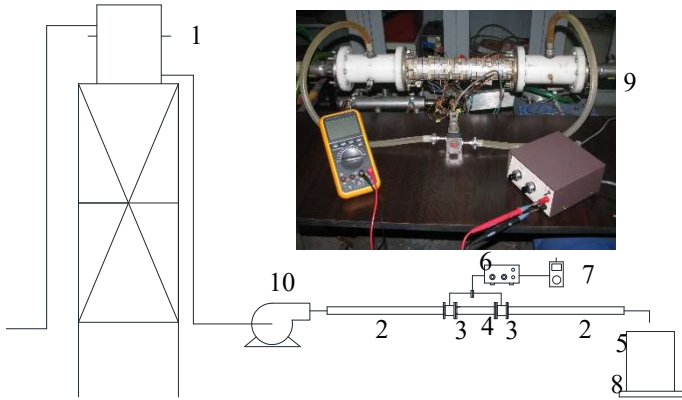


Figure 2. Schematic of experimental setup: 1. supply tank, 2. steel pipe, 3. polyethylene tube, 4. test section, 5. collecting tank, 6. carrier demodulator, 7. multimeter, 8. mass scale, 9. photo of the experimental setup, 10. pump.

For very low flow rates, the pressure drop across the foam sample was too low to accurately measure using the pressure drop diaphragms. A section of packed-spheres porous medium with known pressure drop was added in series with the foam test section. The pressure drop in the foam was obtained using two measurements at each flow rate: 1) pressure drop across the foam and the spheres, and 2) pressure drop across the spheres alone. The pressure drop in the foam was obtained by subtracting the pressure drop in the spheres from the pressure drop in the foam-sphere combination.

Uncertainty in the reported data included error in the directly-measured quantities: length, mass, time and voltage; and propagated error in derived quantities, i.e., flow rate, pressure drop per unit length, reduced pressure drop, Reynolds number and friction factor, Figliola and Beasley [29]. The uncertainties in length and diameter of the metal foam tube were 0.33% and 0.04%, respectively. Three different mass scales were used over the range of flow rates. The precision in the low, medium and large scales were 0.01%, 0.02% and 0.008%, respectively.

As for pressure drop measurements, two sensors were used (each with various diaphragms): DP15 and DP45 with accuracy of $\pm 0.25\%$ and $\pm 0.5\%$ of full scale, respectively. Sensor DP45 with diaphragm 3-24 which could measure up to 2200 Pa was used to obtain data in the Pre-Darcy regime. The uncertainty in the pressure drop sensors was reported by the manufacturer and included effects of linearity, hysteresis and repeatability. The following average estimates were obtained: for the pre-Darcy region, the uncertainty in the pressure drop had a maximum of 1.56%. For all other flow regimes the uncertainty in the measured pressure drop had a maximum of 1.01%. Uncertainty in other derived parameters is reported in the results section.

RESULTS AND DISCUSSION

A plot of the pressure drop over length of the foam vs. average (or Darcy) velocity is shown as Fig. 3. The behavior of the pressure drop is typical for metal foam and for porous media: the pressure drop increases in quadratic fashion with velocity. Quadratic curve fit of the data with a high correlation factor R^2 is shown on the plot.

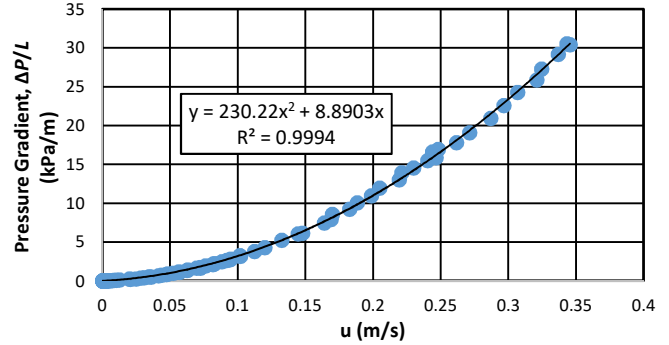


Figure 3. Pressure drop per unit length versus average flow velocity

The pressure drop at the test section with porous media is usually described by the second-order Forchheimer equation:

$$\frac{\Delta p}{L} = \frac{\mu}{K} u + \frac{\rho F}{\sqrt{K}} u^2 \quad (1)$$

where Δp is the static pressure drop, L is the length of the porous medium in the flow direction, μ is the fluid viscosity, and the superficial or Darcy velocity u is calculated by dividing the mass flow rate through the porous medium by the density of the fluid ρ , and the cross-sectional flow area, disregarding the porosity and treating the metal foam tube as if it were hollow. The permeability of the porous medium, K , has units of area and the dimensionless inertia drag coefficient F is known as the Forchheimer coefficient. F is believed to be universal, or at least fixed, for a given class of porous media, [20,21,30]. Both K and F strongly depend on the internal structure of the porous medium. By comparing the curve-fit equation in Fig. 2 to Eq. (1), values of the permeability and Forchheimer coefficient are obtained. These values are listed in the last column of Table 1.

Table 1 Permeability and forchheimer coefficient in various flow regimes

	Darcy Regime	Forchheimer Regime	Turbulent Regime	All Data
Permeability $\times 10^8$ (m ²)	9.89	5.29	34.73	13.16
Forchheimer Coefficient	NA	0.114	0.136	0.133

The choice of dependent variable of Fig. 2, while common, completely hides various flow regimes. The Forchheimer equation can be divided by the average velocity u [2,15,19] to become:

$$\frac{\Delta p}{Lu} = \frac{\mu}{K} + \frac{\rho F}{\sqrt{K}}u \quad (2)$$

Plotting the reduced pressure drop $\Delta p/Lu$ versus velocity would give a straight line for the Forchheimer-regime data. Using the average velocity as an independent variable provides an immediate sense of magnitude of how low or high the water velocity should be in various flow regimes. Fig. 4 is a plot of $\Delta p/Lu$ versus u for all the experimental data. Various flow regimes are discernible by looking at changes in the slope of the reduced pressure drop data.

There is a clear change in the behaviour of the pressure drop around 0.01 to 0.02 m/s. For higher velocities, the reduced pressure drop increases linearly with the velocity indicating that Eq. (2) is satisfied. This first linear behaviour ends around 0.14 m/s, and another linear behaviour starts, but with a slightly different slope. The first linear region is identified as the Forchheimer regime, while the other linear region as the turbulent regime.

In the Forchheimer regime, a permeability value of $5.29 \times 10^{-8} \text{ m}^2$ is obtained by fitting a straight line to the experimental data in this regime. The Forchheimer coefficient obtained is 0.114, which is very different from 0.55—the value well-accepted for packed sphered porous media. In the Forchheimer regime, flow energy dissipation becomes the sum of viscous and form (and inertia) drags. Boundary layers begin to develop near solid boundaries inside the porous medium and they become pronounced and an inertial core appears, [6]. Kinetic energy degradation begins due to pore constrictions (open flow area reduction) and flow direction changes (to go around the ligaments of the foam). Nonetheless, the flow remains laminar and steady. The additional drags are captured by the term that has a second-order dependence on velocity in Eq. (2).

After the end of the Forchheimer regime, the flow becomes turbulent. In the turbulent regime, the pressure drop also satisfies Eq. (2), but with difference coefficients. In the turbulent flow regime, the permeability is $34.73 \times 10^{-8} \text{ m}^2$, and the drag coefficient as 0.136. It is clear that the same foam exhibits different permeabilities and Forchheimer coefficients in different flow regimes. It is also clear that when using the whole data set to calculate the permeability and the Forchheimer coefficient, significantly different values for these properties are obtained, Table 1.

For extremely low velocity, a pre-Darcy regime is identified in Fig. 4 and expanded in Fig. 5. The pre-Darcy regime is not clearly understood and, to the knowledge of the authors, has never been presented in metal foam literature, most likely due to experimental difficulties in accurately measuring the rather small flow rates and pressure drops associated with it. According to Fand et al. [7], in this regime a fluid may exhibit non-Newtonian behavior; and small counter currents along the

pore walls in a direction opposite to the main flow direction may occur. The pre-Darcy regime seems to extend up to about a velocity of 0.004 m/s, after which the Darcy regime begins.

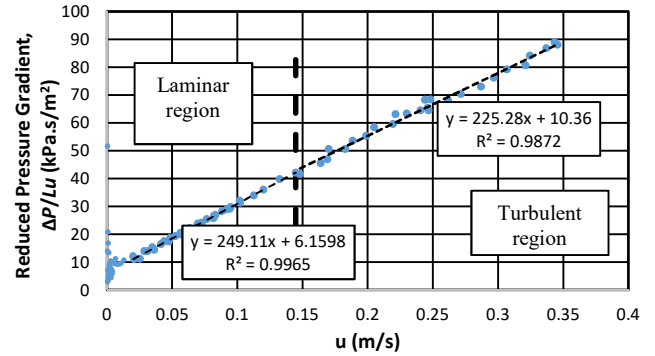


Figure 4. Reduced pressure drop versus average velocity. Uncertainty in reduced pressure drop is 1.11% in the pre-Darcy regime and 0.70% in all other regimes.

The purely viscous Darcy regime is identified by a constant value of the reduced pressure drop, which is identified by a horizontal line corresponding to

$$\frac{\Delta p}{Lu} = \frac{\mu}{K} \quad (3)$$

This Darcy regime prevails for slow flow (creeping or seepage flow); and the pressure drop is solely due to viscous drag. Because of low momentum, the flow engulfs and attaches to the surfaces of the ligaments of the foam. As such, wakes and inertial cores are non-existent, and the actual geometry of the internal structure of the foam is exposed and is directly ‘experienced’ by the flowing fluid. The permeability in this regime is obtained as $9.89 \times 10^{-8} \text{ m}^2$.

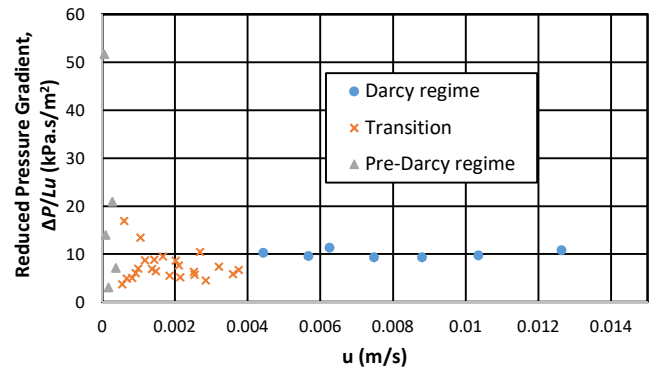


Figure 5. Reduced pressure drop versus average velocity: Darcy and pre-Darcy regimes only. Uncertainty in reduced pressure drop is 1.11% in the pre-Darcy regime and 0.70% in Darcy regime.

Equation (2) can be rearranged in the non-dimensional form:

$$f = \frac{1}{\text{Re}} + F \quad (4)$$

where $f = (\Delta p/L)\sqrt{K}/\rho u^2$ and $Re = \rho u \sqrt{K}/\mu$. Beavers and Sparrow [12] confirmed this relation between for nickel foam; Zhong et al. [22] for sintered stainless-steel foam; while Paek et al. [31], Liu et al. [26] and Mancin et al. [15] confirmed this relation for aluminum foam. Dukhan [32] obtained a similar relation via analysis of Darcy flow including the Brinkman viscous term. As for the coefficient F, it varies among researches: Beavers and Sparrow [12] obtained a value of 0.07; Paek et al. [31] 0.105 and Zhong et al. [22] between 0.41 and 0.75.

Since the same foam exhibits different permeabilities in various flow regimes, a question arises as to which permeability should be used in the definitions of the non-dimensional numbers. Kececioglu and Jiang [8] stressed that the appropriate characteristic length for packed spheres ought to be the square root of the permeability (not the sphere diameter). Boomsma and Poulikakos [19] indicated that Reynolds number based on Darcy-regime permeability was the preferred parameter to indicate transition from Darcy to Forchheimer, since it gave the least divergent values for the three types of metal foam in their study.

The experimental data of the current investigation is plotted in the format of Eq. (4) in Fig. 6. The classical behavior of the friction factor as a function of Reynolds number is displayed.

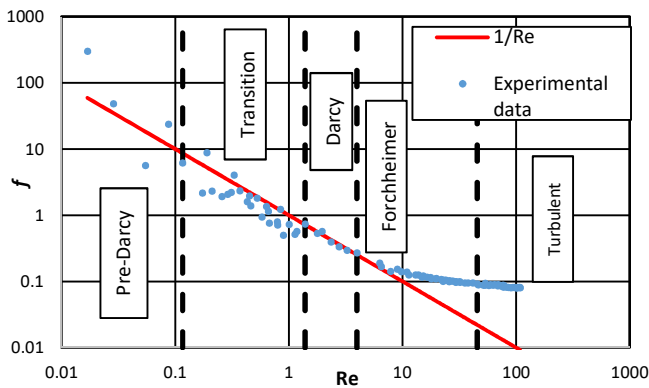


Figure 6. Friction factor versus Reynolds number

Flow regimes are verified by comparing the experimental data to $1/Re$. According to Eq. (4) the data must follow the curve for the Darcy regime; departure from this function signifies the end of the Darcy regime. The departure is seen to occur close to Re between 3 and 6. In the format of Fig. 6, the onset of turbulence is identified when the friction factor becomes independent of Reynolds number. This occurs at around Re equals 46.

CONCLUSION

Results for water flow in high-porosity 10-pore-per-inch commercial open-cell metal foam were presented. Various flow regimes were identified starting with pre-Darcy and ending with turbulent. The same metal foam was seen to exhibit different values of permeability and Forchheimer coefficient in different flow regimes. The square root of the permeability,

measured in the Darcy regime, was used as a length scale for defining Reynolds number and the friction factor. This was seen to correlate the pressure-drop data very well.

ACKNOWLEDGMENTS

This work was supported by the Scientific & Technological Research Council of Turkey (TUBİTAK) under program 1002: 214M267, for which the authors are very thankful.

NOMENCLATURE

- f friction factor (-)
- F Forchheimer coefficient (-)
- K permeability (m²)
- L length of foam in flow direction (m)
- p static pressure (Pa)
- Re Reynolds number based on permeability (-)
- u average (Darcy) flow velocity (m.s⁻¹)

Greek

- Δ change
- μ viscosity (Pa.s)
- ρ density of fluid (kg.m⁻³)

REFERENCES

[1] Dukhan, N., Editor: Metal Foam: Fundamentals and Applications. DESTech, Lancaster, PA 2013.

[2] Antohe, B., Lage, J.L., Price, D.C. and Weber, R.M., Experimental determination of the permeability and inertial coefficients of mechanically compressed aluminum metal layers, *Journal of Fluids Engineering*, Vol. 11, 1997, pp. 404-412.

[3] Tadrist, L., Miscevic, M., Rahli, O. and Topin, F., About the use of fibrous materials in compact heat exchangers, *Experimental Thermal and Fluid Science*, Vol. 28, 2004, pp. 193-199

[4] Boomsma, K., Poulikakos, D. and Zwick, Y., Metal foam as compact high performance heat exchanges, *Mechanics of Materials*, Vol. 35, 2003a, pp. 1161-176.

[5] Ö. Bağcı, N. Dukhan and L. A. Kavurmacioğlu, “Forced-Convection Measurements in the Fully-Developed and Exit Regions of Open-Cell Metal Foam,” *Transport in Porous Media*, DOI: 10.1007/s11242-015-0534-5, Vol. 109, No. 2, 2015, pp. 513-526.

[6] Dybbs, A. and Edwards, R.V., A new look at porous media fluid mechanics – Darcy to turbulent, in *Fundamentals of Transport Phenomena in Porous Media*, J. Bear and M. Y. Corapciolu (Eds.), Martinus Nijhoff Publishers, NATO ASI Series, Series E. The Hague. (1984)

[7] Fand, R.M., Kim, B.Y.Y., Lam, A.C.C., and Phan, R.T., Resistance to the flow of fluids through simple and complex porous media whose matrices are composed of randomly packed spheres, *J. Fluids Eng.*, Vol. 109, 1987, pp. 268-273

[8] Kececioglu, I. and Jiang, Y., Flow through porous media of packed spheres saturated with water, *J. Fluids Eng.*, Vol. 116, 1994, pp.164-170

[9] McDonald, I.F., El_sayed, M.S., Mow, K., and Dullien, F.A.L., Flow through porous media—the Ergun equation

- revisited, *Ind. Eng. Chem. Fundam.*, Vol. 18, No. 3, 1997, pp. 199-208
- [10] Seguin, D., Montillet, A., Comiti, J., Experimental characterization of flow regimes in various porous media—I: Limit of laminar flow regime, *Chem. Eng. Sci.*, Vol. 53, 1998a, pp. 3751-3761
- [11] Seguin, D., Montillet, A., Comiti, J., Huet, F., Experimental characterization of flow regimes in various porous media—II: Transition to turbulent regime, *Chem. Eng. Sci.*, 53, 1998b, pp. 3897-3909
- [12] Beavers, G.S. and Sparrow, E.M., Non-Darcy flow through fibrous porous media, *Journal of Applied Mechanics*, Vol. 36, 1969, pp.711-714
- [13] Montillet, A., Comiti, J. and Legrang, J. Determination of structural parameters of metallic foams from permeametry measurements, *Journal of Material science*, Vol. 27, 1992, pp. 4460-4464
- [14] Edouard, D., Lacroix, A., Huu, C.P. and Luck, F., Pressure drop modeling on solid foam: State of the art correlation, *Chemical Engineering Journal*, Vol. 144, 2008, pp. 299-311
- [15] Mancin, S., Zilio, C., Cavallini, A. and Rossetto, L., Pressure drop during air flow in aluminum foam, *International Journal of Heat and Mass Transfer*, Vol. 53, 2010, pp. 3121-3130
- [16] Kim, S.Y., Paek, J.W. and Kang, B.H., Flow and heat transfer correlations for porous fin in a plate-fin heat exchanger. *Journal of Heat Transfer*, Vol. 122, 2000, pp. 572-578
- [17] Bhattacharya, A., Calmidi, V.V. and Mahajan, R.L., Thermophysical properties of high porosity metal foams, *International Journal of Heat and Mass Transfer*, Vol. 45, 2002, pp. 1017-1031.
- [18] Boomsma, K., Poulikakos, D. and Ventikos, Y., Simulation of flow through open cell metal foams using an idealized periodic cell structure, *International Journal of Heat and Fluid Flow*, Vol. 24, 2003b, pp. 825-834.
- [19] Boomsma, K. and Poulikakos, D., The effect of compression and pore size variations on the liquid flow characteristics in metal foams, *Journal of Fluids Engineering*, Vol. 124, 2002, pp. 263-272.
- [20] Hwang, J.J., Hwang, G.J., Yeh, R.H., and Chao, C.H., Measurement of interstitial convective heat transfer and frictional drag for flow across metal foams, *J. Heat Trans.*, Vol. 124, 2002, pp. 120-129
- [21] Dukhan, N. and Patel, K., Effect of sample's length on flow properties of open-cell metal foam and pressure-drop correlations. *J. Porous Mat.*, Vol. 18, No. 6, 2011, pp. 655-665
- [22] Zhong, W., Li, X., Liu, F. and Tao, G., Measurement and correlation of pressure drop characteristics for air flow through sintered metal foam, *Transp. Porous Med*, 2013, DOI 10.1007/s11242-013-0230-2
- [23] Dukhan, N. and Ali, M., Strong wall and transverse size effects on pressure drop of flow through open-cell metal foam, *International Journal of Thermal Science*, Vol. 57, July 2012a, pp. 85-91
- [24] Dukhan, N., Minjeur II, C.A., A two-permeability approach for assessing flow properties in cellular metals, *J. Porous Mat.*, Vol. 18, No. 4, 2011, pp. 417-424
- [25] Bonnet, J-P, Topin, F. and Tadrst, L., Flow laws in metal foams: compressibility and pore size effect, *Transp Porous Med*, Vol. 73, 2008, pp. 233-254
- [26] Liu, J.F., Wo, W.T., Chiu, W.C. and Hsieh, W.H., Measurement and correlation of friction characteristic of flow through foam matrixes, *Experimental Thermal and Fluid Science*, Vol. 30, 2006, pp. 329-336
- [27] Dukhan, N. and Ali, M., On the various flow regimes in open-cell metal foam, *International Journal of Transport Phenomena*, Vol. 13, No. 2, 2012b, pp. 85-97
- [28] N. Dukhan, Ö. Bağcı, M. Özdemir, "Metal Foam Hydrodynamics: Flow Regimes from Pre-Darcy to Turbulent," *International Journal of Heat and Mass Transfer*, Vol. 77, 2014, pp. 114-123.
- [29] Figliola, R., Beasley, D., *Theory and Design for Mechanical Measurements*. John Wiley and Sons, New York (2000)
- [30] Vafai, K. and Tien, C.L., Boundary and inertia effects on flow and heat transfer in porous media, *Int. J. Heat Mass Trans.*, Vol. 25, No. 8, 1982, pp. 1183-1190
- [31] Paek, J.W., Kang, B.H., Kim, S.Y. and Hyun, M., Effective thermal conductivity and permeability of aluminum foam materials, *International Journal of Thermophysics*, Vol. 21, No. 2, 2000, pp. 453-464
- [32] Dukhan, N., Analysis of Brinkman-extended Darcy flow in porous media and experimental verification using metal foam, *Journal of Fluids Engineering*, Vol. 134, No. 7, July 2012. DOI: 10.1115/1.4005678